doi:10.1007/s11589-011-0775-5

Spatial distribution and focal mechanism solutions of the Wenchuan earthquake series: Results and implications*

Chen Cai[1] Chunquan Yu[1,2] Kai Tao[1] Xingping Hu[3] Yuan Tian[1] Hao Zhang[1] Xiaofeng Cui[3] and Jieyuan Ning[1,♣]

[1] *School of Earth and Space Sciences, Peking University, Beijing* 100871, *China*
[2] *Department of Earth, Atmospheric and Planetary Sciences, MIT, Cambridge, MA* 01239, *USA*
[3] *Institute of Crustal Dynamics, China Earthquake Administration, Beijing* 100085, *China*

Abstract We relocate the spatial distribution of the devastating 12 May 2008 Wenchuan earthquake and its aftershocks. The relocation database is obtained from 89 stations deployed by the China Earthquake Administration, including 54 525 seismograms from 1 376 local earthquakes over M_S3.5 between 12 May 2008 and 3 August 2008. The cross-correlation technique used in this paper has greatly improved the relocation precision by giving much more accurate P-wave differential travel-time measurements than those obtained from routinely picked phase onsets. At the same time, we pick P-wave polarity observations of the Wenchuan earthquake series (hereafter referred to as WES) from 1 023 stations in China and 59 IRIS (Incorporated Research Institutions of Seismology) stations. Then, employing a newly developed program CHNYTX, we obtain 83 well-determined focal mechanism solutions (hereafter referred to as FMSs). Based on spatial distribution and FMSs of the WES, we draw following conclusions: (1) The region near the main shock exhibits a buried low-angle northwest-dipping seismic zone with the main shock at its upper end and two conjugated seismic zones dipping southeast with roughly equal dip-angle; (2) The compressional directions of all kinds of FMSs of the WES are subhorizontal, which reflects the dominant stress in this area is compressional; (3) The principal compressional direction of the regional stress around Wenchuan is roughly perpendicular to the strike of Beichuan-Yingxiu fault, while around Qingchuan it is roughly parallel to the strike of Qingchuan fault. In intermediate part of the Longmenshan area, the principal compressional direction of the stress should be in-between; (4) The possibly existed molten materials in the lower crust of Songpan-Garze terrain have small contribution to the local stress state in Longmenshan area. The listric geometries of the Longmenshan faults most probably resulted from subhorizontal compression along NW-SE direction in history.

Key words: **seismotectonics; stress state; relocation; focal mechanism solution; Wenchuan**
CLC number: P315.2 **Document code**: A

1 Introduction

On 12 May 2008, the devastating Wenchuan M_S7.9 earthquake occurred. This event and its aftershocks compose the Wenchuan earthquake series (WES). They caused huge losses in both human life and properties. To mitigate disasters caused by great earthquakes in future, it is necessary to study source properties and triggering mechanisms of the WES, together with the stress field in Longmenshan area.

Spatial distribution and FMSs of the WES are pivotal data that can be used to depict source properties of the events and to reveal the tectonic stress field in Longmenshan area. Furthermore, by relating spatial distribution and FMSs of the WES with geological settings in which the events took place, geoscientists can study the triggering mechanisms of these events and may hopefully predict potential occurrence of future

* **Received** 21 September 2010; **accepted in revised form** 1 January 2010; **published** 10 February 2011.
♣ **Corresponding author. e-mail**: njy@pku.edu.cn

devastating earthquakes.

Preliminary relocation results of the WES were given by Huang et al. (2008), Zhu et al. (2008), Chen et al. (2009a) and Wu et al. (2009). Those results depicted northwest dipping seismic zones which were interpreted as the locations of northwest dipping faults. However, they did not have enough resolution to compare with industry seismic reflection profiles and geological observations (e.g., Jia et al., 2006; Xu et al., 2009; Li et al., 2010a). For confirming former relocation results of the WES and revealing more discernible structures, it is necessary to show more precise relocation results.

Because P-wave first motion polarity (PWFMP) is an unambiguous physical quantity, the FMSs obtained from it have less uncertainty compared with the results obtained from other methods (Kasahara, 1963; Brillinger et al., 1980; Dziewonski et al., 1981; Kanamori and Given, 1981; Lay et al., 1982; Xu et al., 1983; Udias and Buforn, 1988; Dreger and Helmberger, 1993; Hardebeck and Shearer, 2002). As yet CEA and IRIS have supplied well-distributed high quality seismic data and make PWFMP an ideal quantity to determine FMSs (Yu et al., 2009). Preliminary FMSs of the WES employing PWFMP were given by Hu et al. (2008). They concluded that most earthquakes are thrust events. Moreover, Hu et al. (2008) pointed out that there were a few events with different FMSs. Among them, the first group were strike-slip events around Lixian-Xiaoyudong area, the second group were strike-slip events at the northeast end of the WES, the third group were also thrust events but with a principal compressional direction roughly along the strike of Longmenshan fault system. Later, Zheng et al. (2009b) confirmed the results of Hu et al. (2008). However, limited number of FMSs prevented them from showing comprehensive expression of the regional stress state. For further validating these results and fully understanding their geodynamic implications, it is necessary to give more well-determined FMSs.

In this paper, we will firstly show spatial distribution of the WES relocated by double-difference algorithm (HypoDD), in which cross-correlation technique is employed to improve phase picking accuracy. Then we will show more well-determined FMSs of the WES. Accordingly, we will roughly quantify the principal compressional direction of the regional stress and the influence of possibly existed molten materials in the lower crust of Songpan-Garze terrain on the local stress state around Longmenshan area.

2 Relocation of the WES

We relocate the hypocenters of the WES using the double difference method (Waldhauser and Ellsworth, 2000; Waldhauser, 2001). To improve phase picking accuracy, we employ a cross-correlation technique to estimate differential travel times of P waves. These differential travel time measurements are much more accurate than those obtained from routinely picked phase onsets, thus providing high-quality inputs for our relocation. In addition, we follow Huang et al. (2008) to adopt different velocity structures in the two flanks of Longmenshan fault although this disposal has minor improvement for the relative locations of most earthquakes.

The relocation database is obtained from 89 seismic stations deployed by the CEA (Zheng et al., 2009a, 2010), and includes 54 525 seismograms from 1 376 local earthquakes over M_S3.5 between 12 May 2008 and 3 August 2008. Totally we get 80 823 P-wave differential travel times, with the cross-correlation coefficients greater than 0.7.

To assess the reliability of our results, we carry out several tests similar with those done by Lou et al. (2009). Among them, Jackknife test (e.g., Efron, 1982) is the most important one, in which we recomputed event locations using 89 different subsets of recording data, each with one station omitted. Then we use the relocation results from these data subsamples to estimate relocation uncertainty. The 95% confidence intervals in longitude, latitude and depth are all less than 8 km, whereas in EW and NS directions the locations are almost equally controlled and they are a little bit better than in depth direction (see Figure 1).

Similar to former relocation results, this paper shows that the WES mainly occurred on a NE-SW extended seismic zone (refer to Figure 2a). The earthquake number and the energy released by these earthquakes are unevenly distributed along the strike of the seismic zone. Concretely speaking, earthquake energy is focused around Wenchuan and Qingchuan, whereas relatively less energy was released around Pingwu. Besides, there really exists a NW-SE strike seismic zone perpendicularly intersecting the main seismic zone near its southwest end around Lixian. In addition, more structures in the WES are revealed in this paper.

Because the main seismic zone mentioned above is too narrow in map view, vertical profiles are better for displaying the geometrical structures of the WES. Accordingly, Figures 2b–2e show some vertical profiles

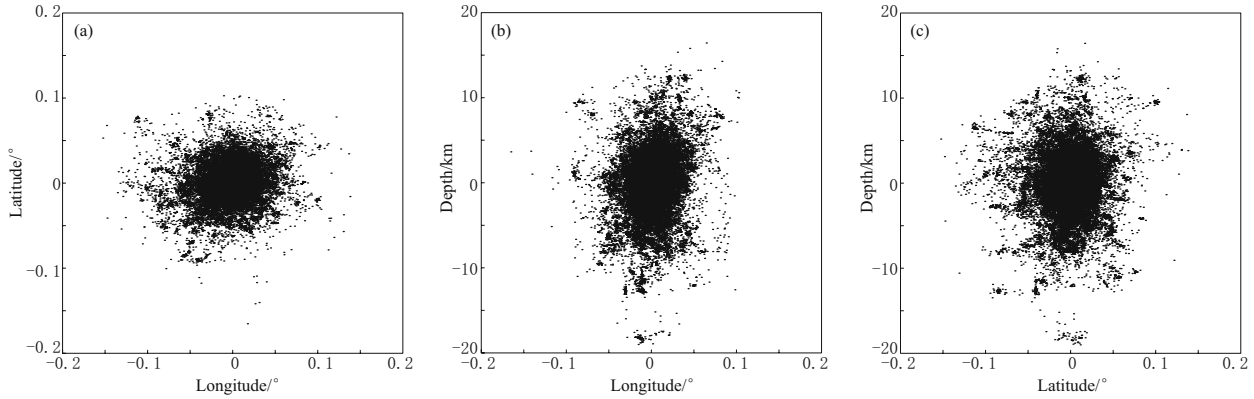

Figure 1 Jacknife uncertainty analysis for relocated events of the Wenchuan earthquake series. 89 subsamples of recording stations were used, each with one station removed, to recompute the locations. The distances shown are deviations from the preferred location (using all stations) for each event. (a) Horizontal profile; (b) North-south profile; (c) East-west profile.

with projection widths 10 km. Among them, profile 7 (Figure 2b) clearly shows a low-angle northwest-dipping seismic zone with the main shock at its upper right (southeast) end. Besides, this seismic zone does not extend to the Earth's surface, obviously leaving a blank zone in shallow depth. Furthermore, we need mention that there are two obviously exhibited conjugated seismic zones besides the northwest-dipping seismic zone in this profile.

Profiles 15 and 32 (Figures 2c–2d) are two vertical profiles further to northeast direction. Although the earthquakes of these two profiles distribute more irregularly compared with profile 7 (Figure 2b), they are not randomly distributed and still show understandable structures. Concretely speaking, there are northwest/southeast dipping seismic zones and vertically distributed seismic zones in profiles 15 and 32 (mainly profile 15), which is to some extent coincident with the geological descriptions that thrust-dominated Beichuan-Yingxiu fault and some NNW-SSE extending strike-slip dominated faults are there (Liu et al., 2009b; Xu et al., 2009; Zhang et al., 2009; Li et al., 2010a). At the same time, we also find indications of horizontally distributed seismic zones in both profile 15 and profile 32 (mainly profile 32), which are in accordance with the inclined seismic zones displayed in Figure 4 and the FMSs described in detail later in this paper.

Profile 37 (Figure 2e) is a vertical profile located near the northeast end of the Longmenshan seismic zone. Different from the three vertical profiles mentioned above, the earthquakes of this profile form three steeply dipped seismic zones, which are expressed as horizontally extended seismic zones in Figure 4 and coincide well with fault structures in this region (Jia et al., 2006), although two horizontally extended seismic zones seem to exist in it and complicate the question.

In summary, the cross-correlation technique employed in this paper has greatly improved the relocation precision as the obtained P-wave differential travel-time measurements are much more accurate than those obtained from routinely-picked phase onsets. As a result, some meaningful structures (e.g., low dip-angle seismic zones, horizontally extended seismic zones) come forth in Figures 2b–2e. Moreover, these structures are consistent well with previous geological/geophysical observations (e.g., Jia et al., 2006; Xu et al., 2009; Zhang et al., 2009; Li et al., 2010a) and the FMSs discussed in the following section.

3 FMSs of the WES

So far, several methods have been developed in determination of P-wave first motion FMSs, which can roughly be classified into two categories: iterative methods (Kasahara, 1963; Brillinger et al., 1980) and grid search methods (GSM) (Udias and Buforn, 1988). The former were less popular than the latter due to its more dependence on data quality. Since 1980s, the latter method has been widely used to determine P-wave first-motion FMSs (Xu et al, 1983; Reasenberg and Oppenheimer, 1985; Hardebeck and Shearer, 2002). It needs to be mentioned that Xu et al. (1983) firstly developed a grid test method (GTM), which can give acceptable solutions in given discrepancy ranges and the mean solutions. Later, Reasenberg and Oppenheimer (1985) put forward a code FPFIT to calculate the best solutions and their confidence intervals. More recently,

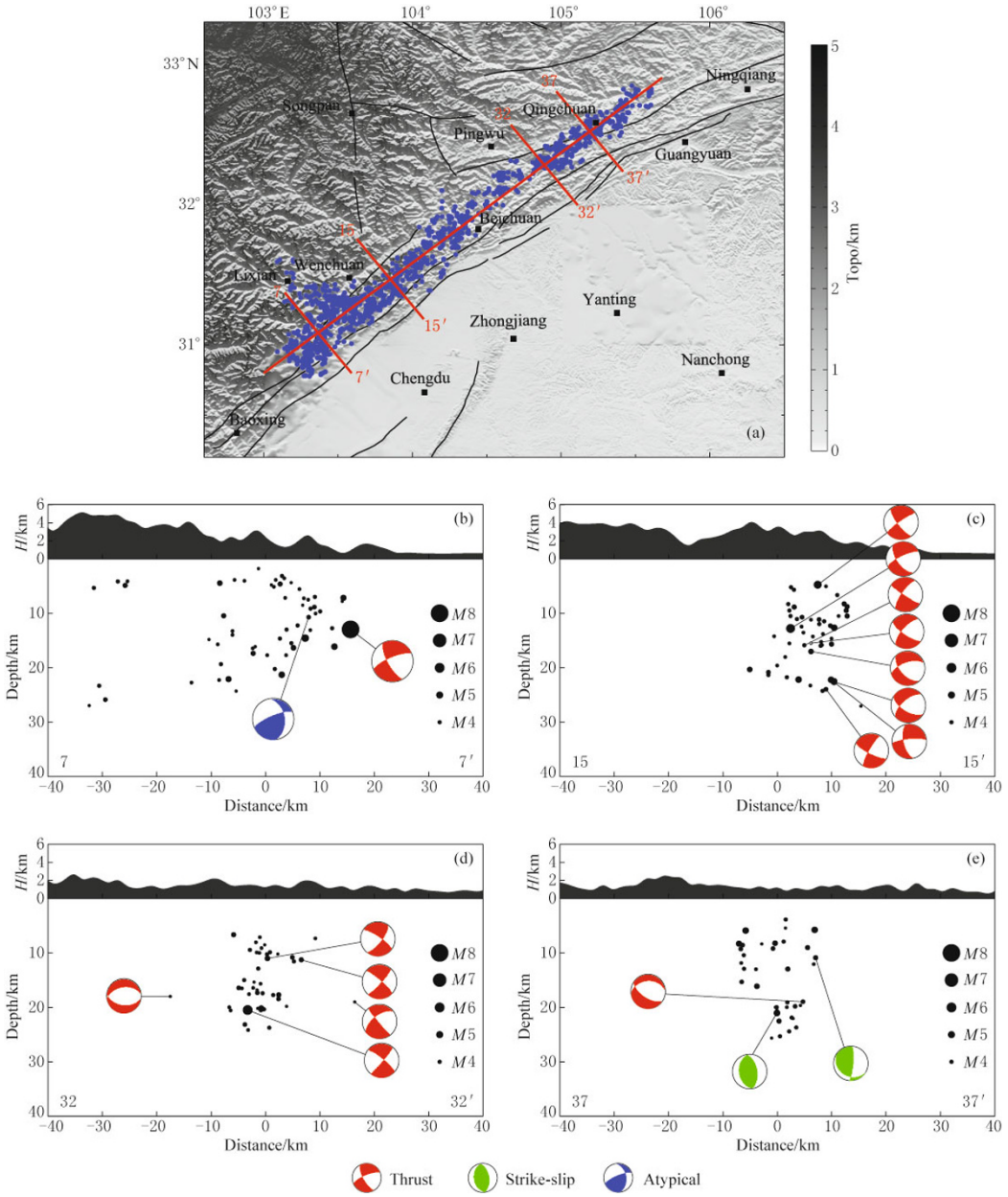

Figure 2 Spatial distribution of relocated earthquakes. (a) Map view display of the WES; (b) Profile 7; (c) Profile 15; (d) Profile 32; (e) Profile 37. In (a), blue dots are earthquakes of the WES, the red short lines with numbers are the locations of the selected four profiles and the red long line is the location of the profile along the main fault. While in (b–e), the beach balls are FMSs with lower hemisphere projection, of which the colored quadrants are extensional quadrants and the white ones are compressional quadrants. Base map with grey color in (a) and the outlines of the black areas atop the vertical profiles in (b–e) express the topography, and the data are from GTOPO30 (http://edc.usgs.gov/products/elevation/gtopo30/gtopo30.html).

Hardbeck and Shearer (2002) also developed a software package HASH.

Although GTM, FPFIT, and HASH were all widely used, they had some drawbacks. First of all, they did not take the distribution of observation points on a focal sphere into consideration in computing inconsistency ratio. Because the inconsistent points on sparsely distributed data areas of a focal sphere are obviously more important than those on densely distributed data areas, it is necessary to weight polarity of the P phases

based upon their distribution density (the number of observation points in a unit area) on a focal sphere. Secondly, FPFIT improperly included a weighting factor which is proportional to the normalized theoretical P-wave amplitude besides the weighting factor reflecting the quality of observations. This weighting scheme was supposed to down-weight obscure observations near nodal planes. However, over suppression on the weight of the data near nodal planes is unnecessary and will tend to select the solutions with more observations near nodal planes. Besides, these methods improperly recommended users to remove isolated solutions and then to obtain a mean solution by simply averaging remaining ones, which might be in danger of losing true solutions.

Meanwhile, there is no satisfactory quality evaluation scheme of FMSs as yet. Mostly, people evaluate the quality of FMSs only by inconsistency ratio, which is not an index to properly evaluate the quality of FMSs. Although FPFIT included some evaluation indices such as NOBS (number of observations), F (minimum misfit) and STDR (station distribution ratio), it ignored the influence of the distribution densities on quality evaluation of FMSs. More importantly, because too many indices prevent people from quantitatively evaluating FMSs, the evaluation scheme of FPFIT could only show qualitative evaluations. For the same reason, although HASH adopted angular difference between two acceptable solutions to evaluate the scatter of FMSs, it still did not keep away from qualitative evaluation when taking many indices of FPFIT into consideration.

Recently, Yu et al. (2009) developed a new GSM program, CHNYTX, which has made a series of improvements. First of all, it adjusted weighting factors in computation of inconsistency ratio by taking the distribution of observation points on a focal sphere into consideration, avoiding over suppression on the weight of the data near nodal planes. Secondly, it employed Jackknife technique to enlarge the acceptable solution set and to improve the inversion quality by adding those acceptable solution subsets, each with one station omitted. Finally, it provided a new scheme for easily evaluating the quality of the FMS using the root-mean-square distance between acceptable solutions and their mean (the distance is measured by the minimum rotation angle) as well as the minimum misfit (the misfit for a given FMS is defined as weighted percentage of the polarity observations that are inconsistent with the predicted polarity for the quadrant in which they appear over all observations). Therefore, this paper employs CHNYTX to determine FMSs of the WES.

We pick up P-wave polarity from 1 023 stations in China. Most of them come from regional networks. The rests are temporary stations installed along the Longmenshan fault a few days after the main shock of the WES. Besides, we also pick up P-wave polarity from 59 IRIS stations, with the epicentral distance ranging from 30° to 90°.

CHNYTX might show more than one cluster of acceptable solutions in general and it was shown by Yu et al. (2009) that at least one cluster of acceptable solutions of an event are very close to the true solution, however, it still needs more knowledge to determine which one is right. For avoiding ambiguity, we only show the well-determined FMSs in this paper. Totally we will introduce 83 FMSs of 83 events.

Among the FMSs of the WES, many are similar with the main shock (see Figure 3). They are thrust events with the principal compressional directions roughly in SE-NW. We name them thrust events of the first type (red beach balls in the southeast of Figure 3 and those on the top of Figure 4). Hu et al. (2008) have already mentioned this kind of earthquakes. In this paper, we clearly show that they distribute unevenly and are mainly accumulated in four places (i.e., close to the main shock, to the north of Wenchuan, around Beichuan, and to the north of Pingwu). Furthermore, we confirm that there is no event with this kind of FMSs at the northeast end of the WES. Besides, the disappearance of these events at the northeast end of the WES is in good agreement with the disappearance of small dip-angle northwestward/southeastward dipping seismic zones in the same region, which is clearly shown in Figure 2e.

Figure 4 shows earthquake distribution as well as FMSs in a vertical profile along the strike of Longmenshan fault. The projection width of this profile is 50 km. From this profile, we can see that the earthquakes mentioned above mostly locate at depths greater than 10 km. All locations with these events do not emerge obliquely-dipped seismic zones in Figure 4 except the place around Xiaoyudong fault, where the NW-SE-trending strike-slip fault intersects the NE-SW-trending Longmenshan fault and forms interference to some extent. Meanwhile, except the earthquake group to the north of Wenchuan, the events with the FMSs of this kind are all gathered in very small depth ranges, and it is further confirmed that they occurred on small dip angle northwestward or southeastward dipping thrust faults. As to the earthquake group to the north of Wenchuan, they probably occurred on four or more small dip-angle thrust faults, which have some indication

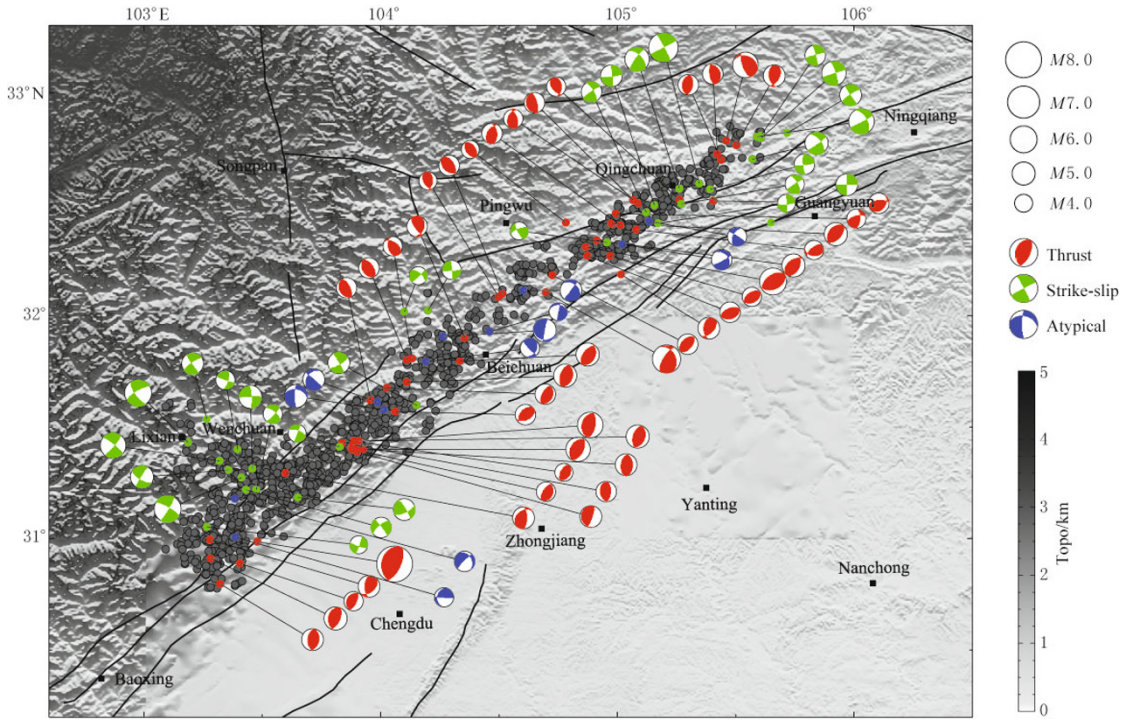

Figure 3 Map view of the earthquake distribution and FMSs of the events. The black circles filled with grey color are relocated events. The beach balls with different colors are FMSs of different kinds. The lower hemisphere projection is adopted in these beach balls, of which the quadrants filled with colors are extensional quadrants and the white ones are compressional quadrants. Base map with grey color also expresses the topography.

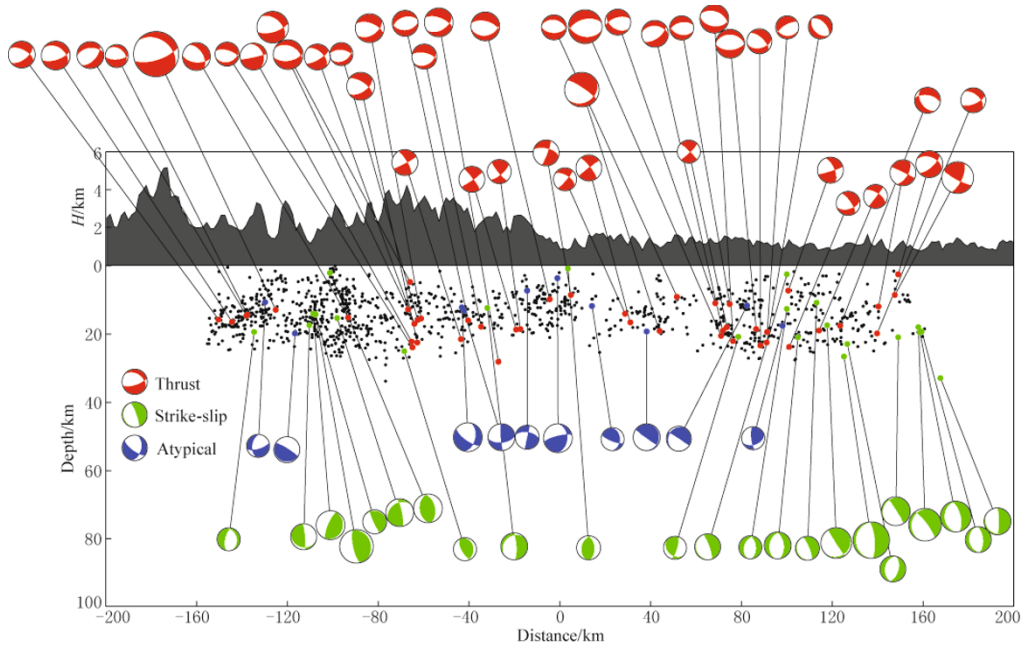

Figure 4 Vertical profile view of the FMSs. Width of the projection profile is 50 km. Black dots are relocated events with no FMSs. Black circles filled with different colors are events with FMSs, which are expressed in the same way as those in Figure 3 except with different projection direction. The outline of the black area at top portion shows the topography.

in Figure 2c. Corresponding to disappearance of small dip-angle northwest or southeast dipping seismic zones in Figure 2e, Figure 4 clearly shows that there exists a small dip angle southwest dipping seismic zone at the right end of the profile, which is in well agreement with the thrust events of the second type introduced in the following paragraph.

We noticed that there are more than ten thrust events with different type of FMSs, of which the principal compressional directions are roughly perpendicular with the ones of the first type and are roughly in NE-SW (red beach balls in the northwest of Figure 3 and those in the low-level row of Figure 4). We name them thrust events of the second type. These events roughly locate to the northwest of the first type. Hu et al. (2008) have already reported the existence of these events although they only found that they emerged to the northeast of Qingchuan. In this paper, we find that this kind of events are distributed in much wider area, i.e., from Beichuan to the northeast end of the WES.

As shown in Figure 4, the thrust earthquakes of the second type at northeast end of the WES are definitely located in a SW-dipping inclined seismic zone with small dip-angle, and those in other places are also possibly located in seismic zones with similar geometry. In addition, these events are all located in the northeastern part of the WES (see Figures 3 and 4), and to the southwest of Beichuan there is almost no event of this type. Inclined seismic zones in Figure 4, the horizontally distributed seismic zones in Figures 2c–2e, and thrust FMSs of the second type mentioned above all mean that there are a series of SW-dipping thrust faults with small dip-angle from Beichuan to the northeast end of the WES. This is also to some extent in accordance with geological observations (e.g., Liu et al., 2009b; Zhang et al., 2009; Li et al., 2010a). Although only a few thrust faults were shown by geologists in western part of the research area, the dip directions of those faults agreed well with the feature revealed in this paper.

Hu et al. (2008) reported strike-slip events around Lixian-Xiaoyudong area and Qingchuan area. In this paper, we further confirm their conclusions. There are about ten events with this type of FMSs respectively around Lixian-Xiaoyudong and Qingchuan, which account for more than about 70% of the total strike-slip events in this area (green beach balls in Figures 3 and 4). And their spatial distribution suggests that they separately locate on left-lateral NW-SE-striking Lixian-Xiaoyudong fault and right-lateral NE-SW-striking Qingchuan fault. Moreover, similar to thrust events of the first type, the focal depths of the strike-slip events are generally very deep, illustrating that the two strike-slip faults are both deep-rooted.

Last but not less important, in middle section of the WES, there are some atypical events (blue beach balls in Figures 2–4) and a few strike-slip events with different principal directions (green beach balls in Figures 2–4). Moreover, these principal directions are not consistent with each other.

4 Discussion and conclusions

This paper relocates the spatial distribution of the WES. The relocation database is obtained from 89 seismic stations deployed by the CEA (Zheng et al., 2009a, 2010), and includes 54 525 seismograms from 1 376 local earthquakes over M_S3.5 between 12 May 2008 and 3 August 2008. The cross-correlation technique employed in this paper has greatly improved the relocation precision as it gives much more accurate P-wave differential travel time measurements than those obtained from routinely picked phase onsets and has supplied high-quality input for relocation processing. As a result, some meaningful structures in seismic zones come forth.

The area near the main shock exhibits a buried low dip-angle northwest dipping seismic zone with the main shock at its upper end and two conjugated seismic zones dipping southeast with roughly equal dip-angle. The area around northeast end of the WES mainly exhibits subvertical seismic zones with NE-SW strike and a low dip angle southwest dipping seismic zone. Whereas the area in middle of the WES is more complex. It seems that there are not only low dip angle northwest/southeast dipping seismic zones, but also subvertical seismic zones. These subvertical zones are located in northwestern part of the WES and might have relation with NNW-SSE trending strike-slip faults around there.

Secondly, we pick P-wave polarity observations of the WES from 1 023 stations in China. Most of them come from regional networks. The rests are temporary stations installed along the Longmenshan fault a few days after the main shock of the WES. Besides, we also pick P-wave polarities from 59 IRIS stations with the epicentral distance from 30° to 90°. Then, based on a newly developed GSM program CHNYTX (Yu et al., 2009), we obtain 83 well-determined FMSs which belong to the WES.

Among these 83 FMSs, there are two types of thrust events. The first type is the type of the main shock. They widely spread in the WES except its northeast end, and their principal compressional directions are roughly in SE-NW. The thrust events of the second type are widely distributed to the north of Beichuan and to the northwest of the first type. Their principal compressional directions are roughly perpendicular to the ones of the first type.

The thrust earthquakes seem to locate in some seismic zones with small dip angles. The dip directions of these seismic zones are also roughly in accordance with the principal compressional directions shown by the FMSs of these events. The compressional directions of all kinds of FMSs are almost subhorizontal. This fact reflects the dominant stress in this area is compressional. The small dip angle characteristics of the seismic zones locating the thrust events further substantiate the reality of the FMSs obtained in this paper. This is totally different from the stress state in the southern part of Sichuan-Yunnan block, which is mainly controlled by extensional stress (Liu et al., 2007).

The coexistence of different types of FMSs might attribute to local variations of rheology. Preexisted strike-slip faults and thrust faults in this area should be produced by the same regional stress. For example, if a place firstly reached its bursting strength (we may call it initial fault), it would break down ahead of other places. At the same time, there would be some faults of different type (we may call them companion faults) accommodating the strain energy if the motion on the initial fault did not gradually attenuate to zero as result of heterogeneity. The initial fault might be thrust fault or strike-slip fault and correspondingly the companion faults might be strike-slip or thrust ones. On the other hand, preexisted strike-slip faults and thrust faults in this area will release energy of different components of the traction acting on them. Namely, the thrust faults tend to release the dip directional component of the traction, while the strike-slip faults tend to release the along-strike component of the traction. As a result, the thrust faults with NE-SW/NW-SE strike, and the strike-slip faults with NE-SW/NW-SE strike in this area would all be activated, which are the cases shown by the geological observations (e.g., Zhang et al., 2009) and the FMSs obtained in this paper.

Independent existence of the first-type events at southwest end of the WES and disappearance of these events at northeast end of the WES roughly quantify the principal compressional direction of the regional stress in this area. Namely, the principal compressional direction of the regional stress around Wenchuan is roughly perpendicular to the strike of Beichuan-Yingxiu fault, while around Qingchuan it is roughly parallel to the strike of Qingchuan fault. Obviously, the principal compressional direction of the stress in intermediate part of the Longmenshan area should be in-between. This feature agrees with the local variation of the tectonic stress given by other results (Xu et al., 1992; Cui and Xie, 1999; Xie et al., 1999; Liu et al., 2007).

Spatial distribution and FMSs of the WES given in this paper can help us study the mechanical role played by possibly existed molten materials in the lower crust of Songpan-Garze terrain. Previous industry seismic reflection profiles and geological observations have proved that the Beichuan-Yingxiu fault and the Hanwang fault in shallower depth are subvertical and it is claimed that these faults at Wenchuan area are listric (e.g., Jia et al., 2006; Xu et al., 2009; Zhang et al., 2009; Li et al., 2010a).

The steeply dipping features of these faults in shallow depth attracted great attention from geoscientists (e.g., Zhou and He, 2009; Zhang et al., 2010). Zhou and He (2009) thought those features might be results of pore fluid in faults, but they cannot explain the new fact given in this paper that there is indeed almost no thrust-event in shallow depth. Zhang et al. (2010) attributed them to products of differential uplift, which implies that the possibly existed molten material in the lower crust of Songpan-Garze terrain has contribution to local stress state (Royden et al., 2008; Teng et al., 2008; Hubbard and Shaw, 2009). Their explanation also contradicts with the facts obtained in this paper that the dip angle of the seismic zone with the main shock in it is small, there is no thrust-event occurred in shallow depth, and the stress state is characterized by a sub-horizontal compression.

Although the evidences shown in this paper cannot totally deny the existence of molten materials in the lower crust of Songpan-Garze terrain, they at least mean that those materials have small contribution to the local stress state in Longmenshan area. At the same time, we claim that the listric geometries of the Longmenshan faults most probably resulted from subhorizontal compression along NW-SE direction in history. Hard crust of the Sichuan block (Zhou and He, 2009; Guo et al., 2009; Liu et al., 2009a; Li et al., 2010b) tends to bend the former low dip-angle straight faults upward and helps to form listric faults. Most probably the faults in shallower depth were broken in advance

of the 12 May 2008 Wenchuan earthquake. Reason is that a larger differential stress near the Earth's surface will be produced when horizontal compressional stress is acted. Meanwhile, reservoir triggered earthquakes occurred at shallower depth could play similar role (Zhou et al., 2010).

Spatial distribution and FMSs of the WES can also help us to predict the potential of devastating events in the future to some extent. Songpan-Garze terrain roughly forms a trapezoidal region with Longmenshan fault as its base. Because the driving force is mainly from the Indian Plate, geometrical spreading leads to fan-shaped trajectories of the compressional direction and decreasing in the value of compressional stress from southwest to northeast in eastern margin of the Tibetan Plateau (Cui and Xie, 1999; Xie et al., 1999; Xu, 2001; Liu et al., 2007).

If the Songpan-Garze terrain were a triangle region, the two sides (Xianshuihe fault and Kunlun fault) would be respectively left-lateral and right-lateral strike-slip faults and there would be less force transferred directly to Longmenshan fault when the two sides were activated. However, Songpan-Garze terrain is trapezoid and both sides are left-lateral. As a result, the earthquakes occurred on Kunlun faults have triggering role on the earthquakes occurred on Longmenshan faults. However, there might exist triangle regions with different dimensions inside the Songpan-Garze terrain roughly from Beichuan to Pingwu. When much energy was released by their sides, stress level on the base would be small and there would be less seismicity. This feature has already been shown before and is further confirmed by this paper that elastic energy was mainly released by the earthquakes around Wenchuan and Qingchuan (e.g., Chen et al., 2009b; Liu et al., 2009b). Meanwhile, FMSs in this area are special (some atypical events as well as a few strike-slip events with different principal directions) and also mean that the stress level is relatively low. Accordingly, we propose that the place with low seismicity roughly from Beichuan to Pingwu might not be the site of the next devastating earthquake in the near future.

Acknowledgements Thanks are given to Profs. Zhonghuai Xu, Shiyong Zhou, Xiufen Zheng, and Fenglin Niu for helpful suggestions. The broadband data used in this paper are supplied by the data backup centre of the CEA. GMT (Wessel and Smith, 1998) is used in the visualization of this paper. This work was supported by the Wenchuan Fault Scientific Drilling Program (WFSD), the Key Projects in the National Science and Technology Pillar Program during the Eleventh Five-year Plan Period under grant No. 2008BAC38B02-4 and the National Natural Science Foundation of China under grant No. 40821062. We would like to acknowledge all the people who helped us in completion of this paper.

References

Brillinger D R, Udias A and Bolt B A (1980). A probability model for regional focal mechanism solutions. *Bull Seismol Soc Am* **70**(1): 149–170.

Chen J H, Liu Q Y, Li S C, Guo B, Li Y, Wang J and Qi S H (2009a). Seismotectonic study by relocation of the Wenchuan M_S8.0 earthquake sequence. *Chinese J Geophys* **52**(2): 390–397 (in Chinese with English abstract).

Chen Z L, Zhao C P, Wang Q C, Hua W, Zhou L Q, Shi H X and Chen H L (2009b). A study on the occurrence background and process of Wenchuan M_S8.0 earthquake. *Chinese J Geophys* **52**(2): 455–463 (in Chinese with English abstract).

Cui X F and Xie F R (1999). Preliminary research to determine stress districts from focal mechanism solutions in Southwest China and its adjacent area. *Acta Seismologica Sinica* **12**(5): 562–572.

Dreger D S and Helmberger D V (1993). Determination of source parameters at regional distances with three-component sparse network data. *J Geophys Res* **98**(B5): 8 107–8 125.

Dziewonski A M, Chou T A and Woodhouse J H (1981). Determination of earthquake source parameters from waveform data for studies of global and regional seismicity. *J Geophys Res* **86**(B4): 2 825–2 852.

Efron B (1982). *The Jackknife, the Bootstrap, and Other Resampling Plans*. SIAM, Philadelphia, 92.

Guo B, Liu Q Y, Chen J H, Liu L S, Li S C, Li Y, Wang J and Qi S H (2009). Teleseismic P-wave tomography of the crust and upper mantle in Longmenshan area, west Sichuan. *Chinese J Geophys* **52**(2): 346–355 (in Chinese with English abstract).

Hardebeck J L and Shearer P M (2002). A new method for determining first-motion focal mechanism. *Bull Seismol Soc Am* **92**(6): 2 264–2 276.

Hu X P, Yu C Q, Tao K, Cui X F, Ning J Y and Wang Y H (2008). Focal mechanism solutions of Wenchuan earthquake and its strong aftershocks obtained from initial P wave polarity analysis. *Chinese J Geophys* **51**(6): 1 711–1 718 (in Chinese with English abstract).

Huang Y, Wu J P, Zhang T Z and Zhang D N (2008). Relocation of the M_S8.0 Wenchuan earthquake and its aftershock sequence. *Science in China* (*Series D*) **38**(10): 1 242–1 249 (in Chinese).

Hubbard J and Shaw J H (2009). Uplift of the Longmen Shan

and Tibetan Plateau, and the 2008 Wenchuan (M=7.9) earthquake. *Nature* **458**: 194–197.

Jia D, Wei G Q, Chen Z X, Li B L, Zeng Q and Yang G (2006). Longmen Shan fold-thrust belt and its relation to the western Sichuan Basin in central China: New insights from hydrocarbon exploration. *AAPG Bulletin* **90**(9): 1 425–1 447.

Kanamori H and Given J W (1981). Use of long-period surface waves for rapid determination of earthquake source parameters. *Phys Earth Planet Int* **27**: 8–31.

Kasahara K (1963). Computer program for a fault-plane solution. *Bull Seismol Soc Am* **53**(1): 1–13.

Lay T, Given J W and Kanamori H (1982). Long-period mechanism of the 8 November 1980 Eureka, California, earthquake. *Bull Seismol Soc Am* **72**(2): 439–456.

Li C Y, Wei Z Y, Ye J Q, Han Y B, Zheng W J (2010a). Amounts and styles of coseismic deformation along the northern segment of surface rupture, of the 2008 Wenchuan M_W 7.9 earthquake, China. *Tectonophysics* **49**: 35–58.

Li Y, Yao H J, Liu Q Y, Chen J H, van der Hilst R D, Li S C, Huang H, Guo B, Wang J and Qi S H (2010b). Phase velocity array tomography of Rayleigh waves in western Sichuan from ambient seismic noise. *Chinese J Geophys* **53**(4): 842–852 (in Chinese with English abstract).

Liu P J, Diao G L and Ning J Y (2007). Fault plane solutions in Sichuan-Yunnan rhombic block and their dynamic implications. *Acta Seismologica Sinica* **20**(5): 479–488.

Liu Q Y, Li Y, Chen J H, Guo B, Li S C, Wang J, Zhang X Q and Qi S H (2009a). Wenchuan M_S8.0 earthquake: preliminary study of the S-wave velocity structure of the crust and upper mantle. *Chinese J Geophys* **52**(2): 309–319 (in Chinese with English abstract).

Liu-Zeng J, Zhang Z, Wen L, Tapponnier P, Sun J, Xing X, Hu G, Xu Q, Zeng L, Ding L, Ji C, Hudnut K W and van der Woerd J (2009b). Co-seismic ruptures of the 12 May, 2008, M_S8.0 Wenchuan earthquake, Sichuan: East-west crustal shortening on oblique, parallel thrusts along the eastern edge of Tibet. *Earth Planet Sci Lett* **286**: 355–370.

Lou X T, Cai C, Yu C Q and Ning J Y (2009). Intermediate-depth earthquakes beneath the Pamir-Hindu Kush Region: evidence for collision between two opposite subduction zones. *Earthquake Sicence* **22**: 659–665.

Reasenberg P and Oppenheimer D (1985). FPFIT, FPPLOT, and FPPAGE: FORTRAN computer programs for calculating and displaying earthquake fault-plane solutions. *U.S. Geol. Surv. Open File Rept.* 85-739, 109pp.

Royden L H, Burchfiel B C and van der Hilst R D (2008). The geological evolution of the Tibetan Plateau. *Science* **321**: 1 054–1 058.

Teng J W, Bai D H, Yang H, Yan Y F, Zhang H S, Zhang Y Q and Ruan X M (2008). Deep processes and dynamic responses associated with the Wenchuan M_S8.0 earthquake of 2008. *Chinese J Geophys* **51**(5): 1 385–1 402 (in Chinese with English abstract).

Udias A and Buforn E (1988). Single and joint fault-plane solutions from first-motion data. In: Doornbos D J ed. *Seismological Algorithms*. Academic Press, London, 443–453.

Waldhauser F (2001). HypoDD: A program to compute double-difference hypocenter locations. *U.S. Geol. Surv. Open File Rept.* 01-113, 25pp.

Waldhauser F and Ellsworth W L (2000). A double-difference earthquake location algorithm: method and application to the Northern Hayward Fault, California. *Bull Seismol Soc Am* **90**(6): 1 353–1 368.

Wessel P and Smith W H F (1998). New, improved version of the Generic Mapping Tools Released. *Eos Trans AGU* **79**: 579.

Wu J P, Huang Y, Zhang T Z, Ming Y H and Fang L H (2009). Aftershock distribution of the M_S8.0 Wenchuan earthquake and three dimensional P-wave velocity structure in and around source region. *Chinese J Geophys* **52**(2): 320–328 (in Chinese with English abstract).

Xie F R, Zhang S M, Dou S Q, Cui X F and Shu S B (1999). Evolution characteristics of quaternary tectonic stress field in the north and east margin of Qinghai-Xizang plateau. *Acta Seismologica Sinica* **12**(5): 550–561.

Xu X W, Wen X Z, Yu G H, Chen G H, Klinger Y, Hubbard J and Shaw J (2009). Coseismic reverse- and oblique-slip surface faulting generated by the 2008 M_W7.9 Wenchuan earthquake, China. *Geology* **37**(6): 515–518.

Xu Z H (2001). A present-day tectonic stress map for eastern Asia region. *Acta Seismologica Sinica* **14**(5): 524–533.

Xu Z H, Wang S Y, Huang Y R and Gao A J (1992). Tectonic stress field of China inferred from a large number of small earthquakes. *J Geophy Res* **97**(B8): 11 867–11 877.

Xu Z H, Yan M and Zhao Z H (1983). Evaluation of the direction of tectonic stress in north China from recorded data of a large number of small earthquakes. *Acta Seismologica Sinica* **5**(3): 268–279 (in Chinese with English abstract).

Yu C Q, Tao K, Cui X F, Hu X P and Ning J Y (2009). P-wave first-motion focal mechanism solutions and their quality evaluation. *Chinese J Geophys* **52**(5): 1 402–1 411 (in Chinese with English abstract).

Zhang P Z, Wen X Z, Xu X W, Gan W J, Wang M, Shen Z K, Wang Q L, Huang Y, Zheng Y, Li X J, Zhang Z Q, Ma S L, Ran Y K, Liu Q Y, Ding Z F and Wu J P (2009). Tectonic model of the great Wenchuan earthquake of May 12, 2008, Sichuan, China. *Chinese Science Bulletin* **54**(7): 944–953 (in Chinese)

Zhang Z Q, Zhang P Z and Wang Q L (2010). The structure and seismogenic mechanism of Longmenshan high dip-angle reverse fault. *Chinese J Geophys* **53**(9): 2 068–2 082 (in Chinese with English abstract).

Zheng X F, Ouyang B, Zhang D N, Yao Z X, Liang J H

and Zheng J (2009a). Technical system construction of data backup center for China seismograph network and the data support to researchers on the Wenchuan earthquake. *Chinese J Geophys* **52**(5): 1 412–1 417 (in Chinese with English abstract).

Zheng X F, Yao Z X, Liang J H and Zheng J (2010). The role played and opportunities provided by IGP DMC of China National Seismic Network in Wenchuan earthquake disaster relief and researches. *Bull Seismol Soc Am* **100**(5B): 2 866–2 872.

Zheng Y, Ma H S, Lü J, Ni S D, Li Y C and Wei S J (2009b). Source mechanism of strong aftershocks (M_S5.6) of the 2008/05/12 Wenchuan earthquake and the implication for seismotectonics. *Science in China* (*Series D*) **52**(6): 739–753.

Zhou B, Xue S F, Deng Z H, Sun F, Jiang H K, Zhang X D and Lu X (2010). Relationship between the evolution of reservoir-induced seismicity in space-time and the process of reservoir water body load-unloading and water infiltration: a case study of Zipingpu reservoir. *Chinese J Geophys* **53**(11): 2 651–2 670.

Zhou Y S and He C R (2009). The rheological structures of crust and mechanics of high-angle reverse fault slip for Wenchuan M_S8.0 earthquake. *Chinese J Geophys* **52**(2): 474–484 (in Chinese with English abstract).

Zhu A L, Xu X W, Diao G L, Su J R, Feng X D, Sun Q and Wang Y L (2008). Relocation of the M_S8.0 Wenchuan earthquake sequence in part: preliminary seismotectonic analysis. *Seismology and Geology* **30**(3): 759–767 (in Chinese with English abstract).